Sequence-based Decoupling Encoder for Well Log Interpretation

Ning Qian[1], Yiming Xu[1], Monika Sester[1]

[1] Institute of Cartography and Geoinformatics, Leibniz Universität Hannover, Germany
(ning.qian, yiming.xu, monika.sester)@ikg.uni-hannover.de

Keywords: Well log interpretation, Self-attention, Sequence-based, Decoupling.

Abstract

Well logging curves play a crucial role in oil and gas exploration and geological engineering, as they provide essential information about subsurface formations and reservoir properties. In recent years, with the growing adoption of deep learning techniques in geoscientific data analysis, well logging data have increasingly been modeled as depth-dependent sequences, enabling the application of sequential neural networks for their analysis. Among these approaches, attention mechanisms have been adopted in log interpretation tasks due to their ability to capture long-range dependencies within sequences. However, directly applying attention mechanisms without considering the intrinsic structure of logging data may introduce model redundancy and increase learning complexity, which can ultimately degrade predictive performance. To address this issue, this study proposes a Sequence-based Decoupling Encoder (SDE). The proposed encoder explicitly disentangles the interactions between logging curves and across depth, enabling the model to learn relationships along different dimensions separately, which allows more effective feature extraction and mapping into a latent space. The decoupling strategy also reduces the learning complexity of the attention mechanism and provides clearer learning objectives for the model. The proposed method is evaluated on the public dataset *FORCE2020* and applied to two common well log interpretation tasks: missing log reconstruction and lithology prediction. We compare SDE against several representative sequential baselines. Experimental results demonstrate that SDE achieves superior predictive performance in both tasks.

1. Introduction

Well log data provide one of the most important sources of subsurface information for hydrocarbon exploration, reservoir characterization, and geological engineering. Acquired along boreholes, several logging curves continuously measure the physical responses of subsurface formations and are widely used for lithology interpretation and formation evaluation. Traditionally, lithological interpretation has relied heavily on expert analysis, making it time-consuming and labor-intensive. To improve interpretive efficiency, machine learning techniques are increasingly used for automated lithological identification and well log analysis. However, effectively modeling the depth sequence structure and multi-curve interactions of well log data remains a challenging problem.

In practical applications, well log datasets are often incomplete due to variations in acquisition conditions. Different wells may record different types of logging curves depending on the logging tools, operational constraints, or economic considerations. In addition, sensor failures, borehole conditions, and environmental noise can further result in missing or corrupted measurements. As a consequence, real-world well log datasets commonly exhibit significant missing values across both depth and curve dimensions. Traditional approaches typically address this issue through statistical imputation methods, such as mean or median filling, or by applying interpolation techniques. However, these strategies may oversimplify the underlying geological variations and introduce biased or overly smooth representations.

With the rapid development of deep learning, sequence modeling approaches provide a promising alternative for handling incomplete well log data. Instead of explicitly filling missing values, sequence models can implicitly learn feature representations from partially observed data by leveraging contextual dependencies along depth and across logging curves. This enables the model to recover more realistic patterns and capture the intrinsic continuity of subsurface formations.

Nevertheless, existing deep learning methods still face limitations in modeling long-range dependencies and jointly learning cross-depth and cross-curve interactions. In particular, when these interactions are modeled simultaneously, the learning process becomes highly complex, often leading to inefficient representations and overly smooth predictions that fail to capture detailed variations in logging curves.

To address these challenges, we propose a Sequence-based Decoupled Encoder (SDE) that explicitly separates cross-depth and cross-curve interactions during representation learning. The core idea is to decouple the attention mechanism into two complementary components: one component models relationships between different well logging curves, while the other captures sequence dependencies along the depth dimension of individual curves. By separating these interaction spaces, the model can learn more structured representations and better preserve the intrinsic sequential characteristics of well logging data. Moreover, since depth-wise dependencies are closely related to geological processes such as stratigraphic continuity and sedimentary layering, explicitly modeling these relationships enables the encoder to produce more geologically meaningful representations.

The main contributions of this work are summarized as follows:

1. A novel Sequence-based Decoupled Encoder (SDE) is proposed, which explicitly separates cross-depth and cross-curve interactions to better capture sequential correlations in well log data.

2. The proposed method improves reconstruction capability for missing well logs, enabling more realistic curve recovery instead of oversmoothed predictions.

3. The method enhances lithology identification performance, achieving more accurate lithological boundaries and better recognition of minority classes.

4. A generalizable representation learning framework is developed, which can be applied to multiple downstream tasks such as lithology identification and subsurface characterization.

In experiments, the proposed SDE serves as an effective and general representation learning module for well log analysis. Its performance is validated on the *FORCE2020* dataset, demonstrating its effectiveness in tasks including missing log reconstruction and lithology identification reconstruction and lithology identification.

2. Related Works

Early studies employed a variety of traditional machine learning algorithms, including support vector machines (Liang et al., 2022), random forests (Ao et al., 2018), kernel density estimation (Corina and Hovda, 2018), extreme learning machines (Li et al., 2021), and gradient boosting models (Han et al., 2021), to perform lithology classification based on well logging measurements. Furthermore, several hybrid approaches integrating machine learning algorithms with geological constraints or domain-specific features (Li et al., 2024) (Ye et al., 2021) (He et al., 2023) have been developed to improve lithology identification in complex reservoirs. Despite their promising performance, these methods generally rely on handcrafted features and treat logging samples as independent observations, thereby limiting their ability to fully exploit the sequential structure inherent in well log data.

In recent years, deep learning models have been increasingly adopted for the analysis of sequential well logging data. Convolutional Neural Networks (CNNs) (Wang et al., 2020) (Zhang et al., 2025) have been widely applied to automatically extract layered features from logging curves and capture local patterns along the depth dimension. However, the CNN architecture is limited by its fixed receptive field, which makes it difficult to capture long-range dependencies in deep formations. To overcome this limitation, Recurrent Neural Networks (RNNs) (Jiang et al., 2021), including Long Short-Term Memory (LSTM) networks (Shan et al., 2021) and Gated Recurrent Unit (GRU) networks (Zeng et al., 2020), have been introduced to model sequence relationships along the depth dimension. In addition, spatiotemporal deep learning frameworks, such as STNet (Zhao et al., 2022), integrate spatial prediction and multi-scale graph clustering to leverage geological continuity and enhance lithological boundary detection. Despite these advances, sequence models based on convolutional or recurrent architectures still have limitations in capturing global contextual dependencies across long depth intervals and multiple logging curves.

With the Transformer architecture demonstrating its ability to capture long-term dependencies through attention mechanisms, Transformer-based architectures have been applied in well logging analysis (Xu et al., 2023), achieving synchronous feature interactions across depth samples and multiple well logging curves. However, the joint modeling of cross-depth and cross-curve interactions significantly increases the complexity of the learning process. When the model learns relationships in two dimensions simultaneously, the attention mechanism must search for relevant dependencies in a vast multidimensional feature space. This often leads to inefficient representation learning and may result in overly smooth predictions that approximate global trends rather than capturing the true changes in the well logging curves.

3. Methodology

3.1 Sequence-based Decoupling Encoder

Well logging data are characterized by two fundamental structural properties: depth-wise sequential dependency and cross-curve correlation. Previous methods typically model both types of interactions simultaneously in a unified feature space (Xu et al., 2023). In contrast to previous methods, we designed a Sequence-based Decoupling Encoder (SDE) that explicitly separates cross-curve interactions and cross-depth interactions, models the dependencies between the curve dimension and the depth dimension separately, and obtains a unified latent representation through feature fusion. This decoupled learning strategy reduces computational complexity from $O(F^2N^2)$ to $O(F^2) + O(N^2)$, where F is the number of different curves in the log, and N is the length of depth samples. This indicates that the SDE no longer needs to learn interaction information from (F^2N^2) features, but instead learns from (F^2) and (N^2) features separately. Since the attention mechanism requires the model to find the information it needs to pay attention to on its own, simultaneous multi-dimensional interaction will greatly increase the difficulty of model learning. The cross-depth interaction in decoupled learning can help the model to focus on the depth-wise representations of each curve, providing a clearer learning objective and making it a universal encoder for various downstream tasks.

The overall architecture of the encoder is illustrated in Fig. 1. The SDE consists of four main components: local multi-curve embedding, cross-curve interaction, cross-depth interaction and feature fusion. The final latent representation produced by the encoder is then fed into a decoder for downstream prediction tasks.

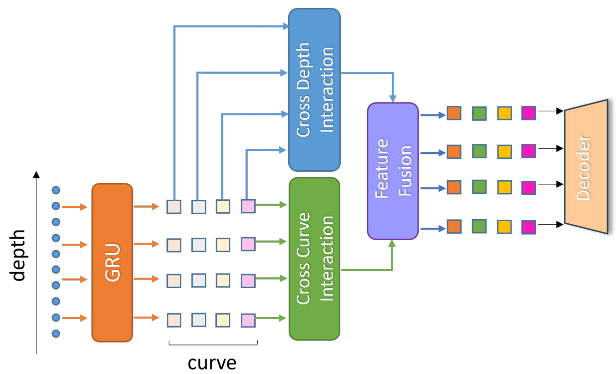

Figure 1. Architecture of the proposed Sequence-based Decoupling Encoder (SDE).

3.1.1 Local Multi-Curve Embedding

In well logs, different curves exhibit significant differences in physical meaning, response mechanism, and numerical distribution characteristics. Therefore, this paper designs a Local Multi-Curve Embedding module. The core idea of this module is to first perform independent local sequence modeling for each curve, and then map the local representations of each curve to a unified latent space for organization and fusion.

The input well logging data is represented as $\mathbf{X} \in \mathbb{R}^{B\times N\times F}$, where B represents the batch size, N represents the number of depth sampling points, and F represents the number of well logging curves. The input also includes a $\mathbf{Mask} \in \{0,1\}^{B\times N\times F}$ to indicate whether the corresponding position is valid. For invalid positions, a learnable mask embedding vector is used to replace them to avoid introducing excessive numerical bias during sequence encoding. We divide the depth dimension into several local windows. For each curve f, we extract its corresponding local block sequence from the masked input tensor $\tilde{E}^{(f)}$, and further reassemble it into:

$$\tilde{E}^{(f)}_{\text{block}} \in \mathbb{R}^{(B\cdot L')\times K\times d}, \tag{1}$$

where d represents the feature dimension, K is the local compression length, and $K \cdot L' = N$. To fully preserve the unique local variation patterns of different logging curves, a Gated Recurrent Unit(GRU) with independent parameters is assigned to each curve. Therefore, the hidden state update of the f-th curve in the l-th local window can be written as follows:

$$h_t^{(f,l)} = f_{\text{GRU}}^{(f)}\left(\tilde{e}_t^{(f,l)},\, h_{t-1}^{(f,l)}\right), \quad t = 1,2,\ldots,K. \tag{2}$$

After GRU encoding is completed, the last hidden state of the last GRU layer is taken as the compressed representation of the local block:

$$z^{(f,l)} = h_K^{(f,l)} \in \mathbb{R}^d. \tag{3}$$

After local encoding is completed for all curves and all local windows, they are stacked along the curve dimension to obtain the local multi-curve embedding output:

$$\mathbf{H}_0 = \text{Stack}\left(Z^{(1)}, Z^{(2)}, \ldots, Z^{(F)}\right) \in \mathbb{R}^{B\times L'\times F\times d}. \tag{4}$$

The original pointwise mask also needs to be reassembled according to the block length K, and max pooling is performed along the window dimension within the block to obtain a local block-level mask. This mask indicates whether a curve has at least one valid observation point within a certain local depth block.

3.1.2 Cross-curve Interaction After local multi-curve embedding is completed, the encoder obtains a block-level feature representation $\mathbf{H}_0 \in \mathbb{R}^{B\times L'\times F\times D}$. Therefore, the goal of cross-curve interaction is to explicitly model the correlation between different curves within a fixed depth block, thereby extracting the complementary response relationship between multiple curves.

To enhance the model’s ability to distinguish different log types, we introduce a learnable curve identity embedding $\mathbf{E}_{\text{curve}} \in \mathbb{R}^{F\times D}$. During forward propagation, the curve embeddings are added to the local multi-curve features. The cross-curve interaction module then performs self-attention along the curve dimension. Specifically, the batch dimension and the local depth block dimension are merged, organizing the F curves within each depth block into a feature sequence of length F:

$$\mathbf{H}_c = \text{SelfAttn}(\mathbf{X}_c + \mathbf{E}_{\text{curve}}), \tag{5}$$

where $\mathbf{X}_c \in \mathbb{R}^{(B\cdot L')\times F\times D}$ denotes the curve-wise feature sequence and $\mathbf{H}_c$ represents the output representation after cross-curve interaction.

This allows the model to learn the relationships between curves independently within each local depth block, without mixing information from different depth blocks. During self-attention, the mask generated above is used for weight masking, ensuring that the model allocates attention weights only between valid curves, avoiding interference from missing curves or invalid observations in modeling curve relationships.

3.1.3 Cross-depth Interaction To explicitly introduce depth order information, positional encoding $\mathbf{P} \in \mathbb{R}^{\mathbb{L}'}$ is added to the features, enabling the attention mechanism to distinguish the relative positional relationships between different depth blocks. Subsequently, multi-head self-attention is applied along the depth dimension:

$$\mathbf{H}_d = \text{SelfAttn}(\mathbf{X}_d + \mathbf{P}), \tag{6}$$

where $\mathbf{X}_d \in \mathbb{R}^{(B\cdot F)\times L'\times D}$ and $\mathbf{H}_d$ denotes the depth-aware representation.

Geologically, the cross-depth interaction module enables the model to capture vertical features such as lithological gradation, sedimentary cycles, and reservoir structure. When the logging response at a certain depth location exhibits similar patterns to other segments, the attention mechanism automatically enhances information propagation between these related locations, resulting in more context-consistent feature representations.

3.1.4 Feature Fusion To integrate the complementary information captured by cross-curve and cross-depth interactions, the outputs of the two branches are added element-wise. Since the features generated by the two branches have the same dimension, their outputs can be directly combined to form a unified representation. Then, the same interaction and fusion process is repeated on the fused features to further enhance the encoder’s representational power and obtain the final fused features.

4. Experiment

4.1 Dataset

The dataset used in this study originates from the FORCE 2020 lithology prediction machine learning competition (Bormann et al., 2020). This dataset contains logging data and lithological interpretations from 118 wells located in the Norwegian North Sea. 98 wells were used for training, 10 for validation, and 10 for testing. The dataset provides various conventional logging data, such as gamma-ray (GR), neutron porosity (NPHI), bulk density (RHOB), resistivity logging (RMED, RDEP), sonic logging (DTC and DTS), photoelectric factor (PEF), spontaneous potential (SP), and some wellbore-related measurements, including caliper (CALI) and differential caliper (DCAL). Lithology labels were manually interpreted by geoscientists and include various rock types, such as sandstone, shale, limestone, chalk, dolomite, marl, anhydrite, halite, coal, and tuff.

4.1.1 Data preprocessing Before model training, several preprocessing steps are applied to the well log data to improve data consistency and facilitate representation learning. Resistivity logging curves (including RSHA, RMED, and RDEP) are transformed using a logarithmic transformation. Due to variations in formation properties, resistivity measurements typically span several orders of magnitude, resulting in a highly skewed data distribution in the original coordinate system. Logarithmic transformation compresses the dynamic range of the data and

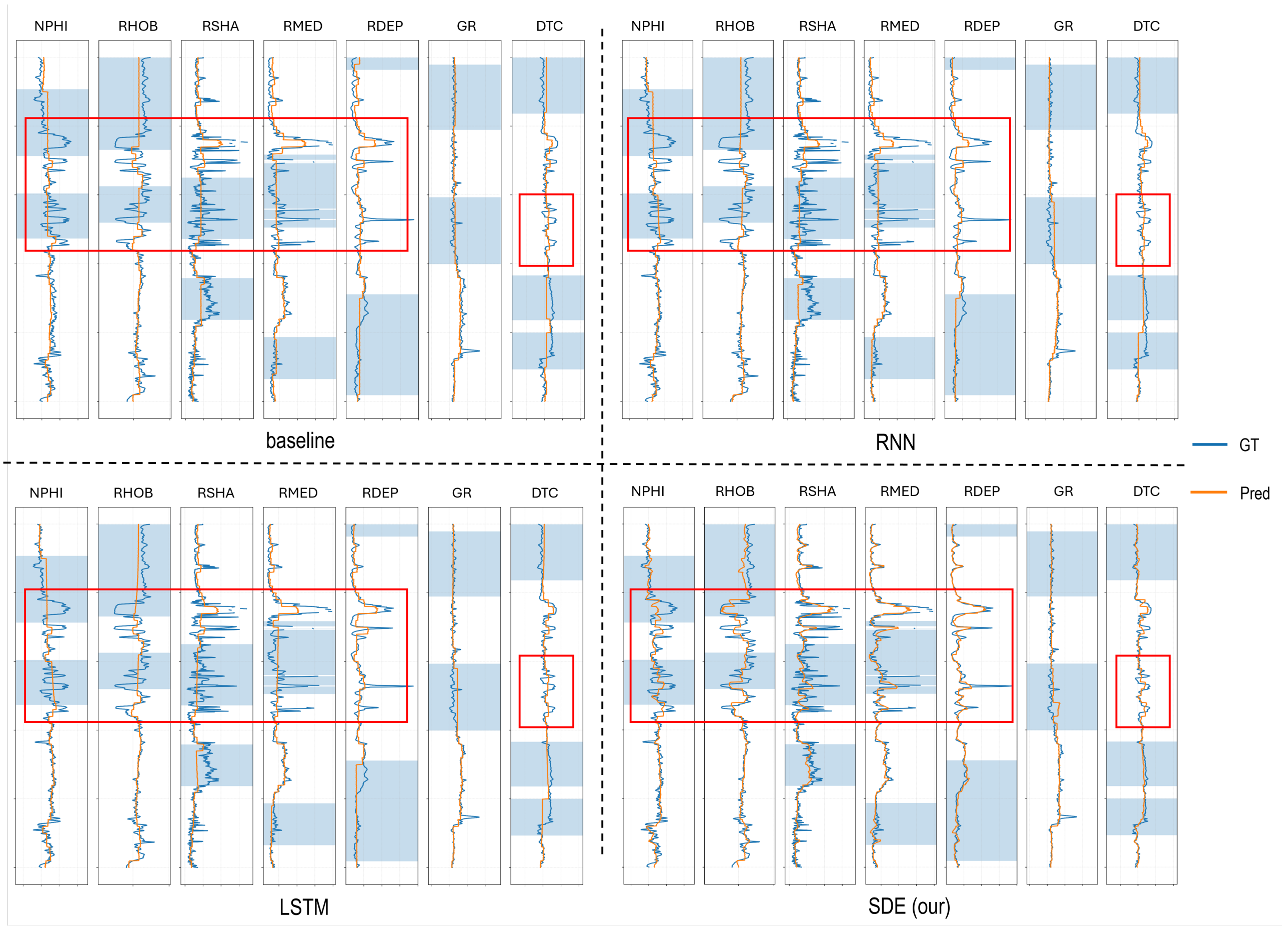

Figure 2. Reconstruction results of well logs obtained using different models. The blue curves represent the ground truth, while the orange curves denote the predicted results. The masked regions, highlighted in light blue, are excluded from the model during the entire training and inference process. Red boxes indicate regions where the proposed method achieves noticeably improved reconstruction performance compared to other approaches.

converts the distribution to a form closer to a normal distribution, thereby improving numerical stability and facilitating model training. Furthermore, z-score normalization is used to standardize all logging measurements to ensure that different logging curves are at comparable numerical scales and to prevent features with large values from dominating the learning process. We employ a sliding window strategy to segment the logging sequences at the well level. Specifically, each well is divided into several subsequences, each with a fixed length of 1000 depth samples and a step size of 800. Here, a depth sample refers to an individual measurement point along the borehole depth at which logging values are recorded. This segmentation strategy increases the number of training samples while maintaining the structure of the logging data sequence.

4.1.2 Missing Logging Data A significant characteristic of the *FORCE2020* dataset is the presence of missing logging data. However, the missing values are not explicitly filled during preprocessing. Instead, a corresponding mask matrix is generated to distinguish between valid and missing observations. In subsequent attention-based interaction processes, these masks are used to prevent missing values from participating in feature interactions, thus ensuring that invalid data does not interfere with the representation learning process.

Method	Params	FLOPs	Latency
Baseline	2.5M	2.29G	24.34ms
SDE (Ours)	**1.1M**	**1.27G**	**19.71ms**

Table 1. Computational complexity comparison between the baseline model and the proposed SDE-based model.

4.2 Computational Complexity Analysis

To further evaluate the efficiency of the proposed model, we compare the computational complexity of the baseline model and the proposed SDE-based model in terms of the number of parameters, floating point operations (FLOPs), and inference latency. The results are summarized in Table 1.

As shown in Table 1, the proposed SDE model achieves a significantly lower computational cost compared with the baseline model. Specifically, the number of parameters is reduced from 2.5M to 1.1M, indicating that the proposed model requires less memory for parameter storage. In addition, the FLOPs decrease from 2.29G to 1.27G, demonstrating that the SDE-based architecture performs fewer arithmetic operations during inference. Correspondingly, the inference latency is reduced from 24.34 ms to 19.71 ms, suggesting that the proposed model can achieve faster prediction speed in practical applications.

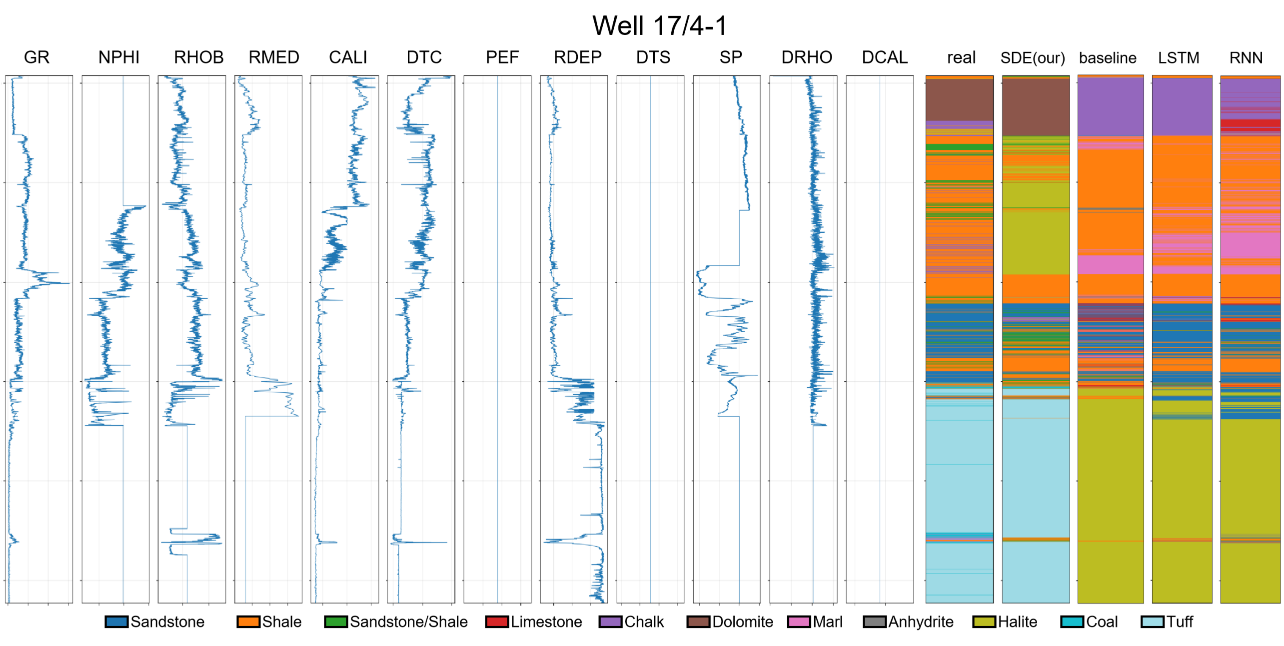

Figure 3. The result of lithology identification of Well 17/4-1.

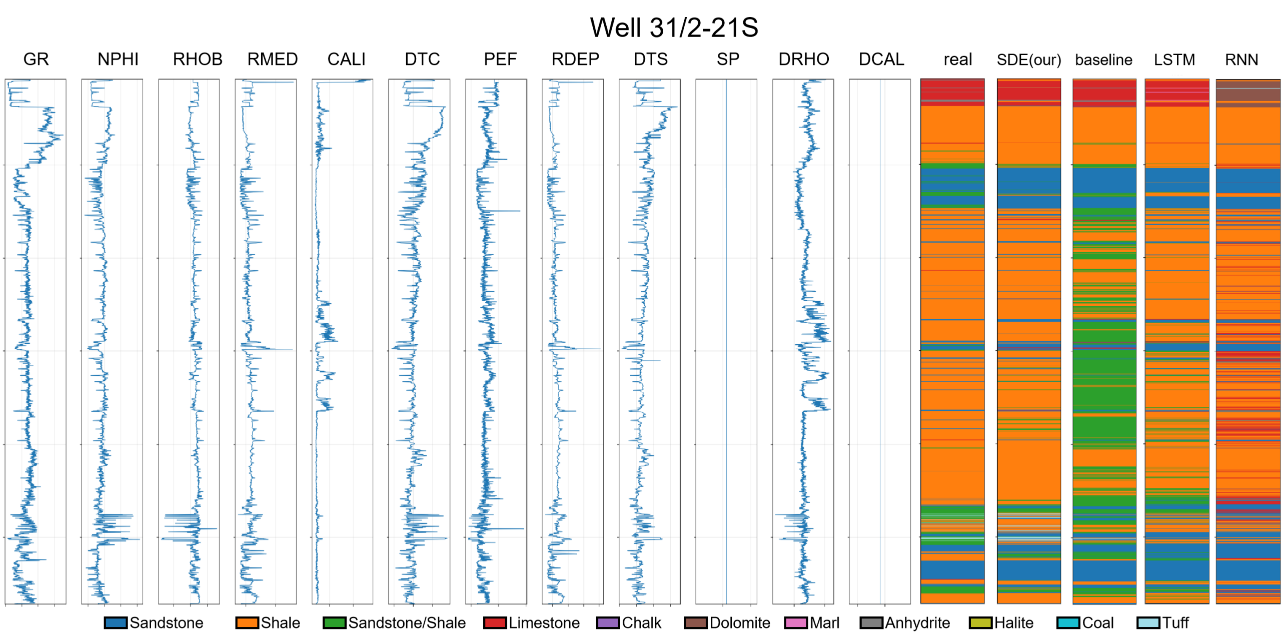

Figure 4. The result of lithology identification of Well 31/2-21 S.

4.3 Results

To evaluate the effectiveness and generalization ability of the proposed representation learning framework, we conducted experiments on two tasks: missing logging curve reconstruction and lithology classification. Both tasks share the same encoder structure but use task-specific Multilayer Perceptron (MLP) decoders to tune the learned representations to suit the different objectives. For a fair comparison, the encoder structure connected to each model remains consistent across different tasks to ensure that performance differences primarily stem from the encoder’s representational capabilities.

Four encoders are evaluated, including a baseline model, RNN, LSTM, and the proposed SDE. The baseline model performs joint interaction modeling over the entire curve–depth feature grid, allowing simultaneous learning of dependencies across both curve and depth dimensions. Specifically, the baseline adopts the Transformer-based encoding architecture proposed in (Xu et al., 2023), in which all input tokens are processed within a unified self-attention framework. This design enables global feature interactions across the curve and depth dimensions, but also increases the complexity of representation learning due to the entangled modeling of heterogeneous dependencies.

4.3.1 Missing Log Reconstruction For the missing log reconstruction task, we employ a masked autoencoder training strategy. Specifically, we progressively apply randomly gener-

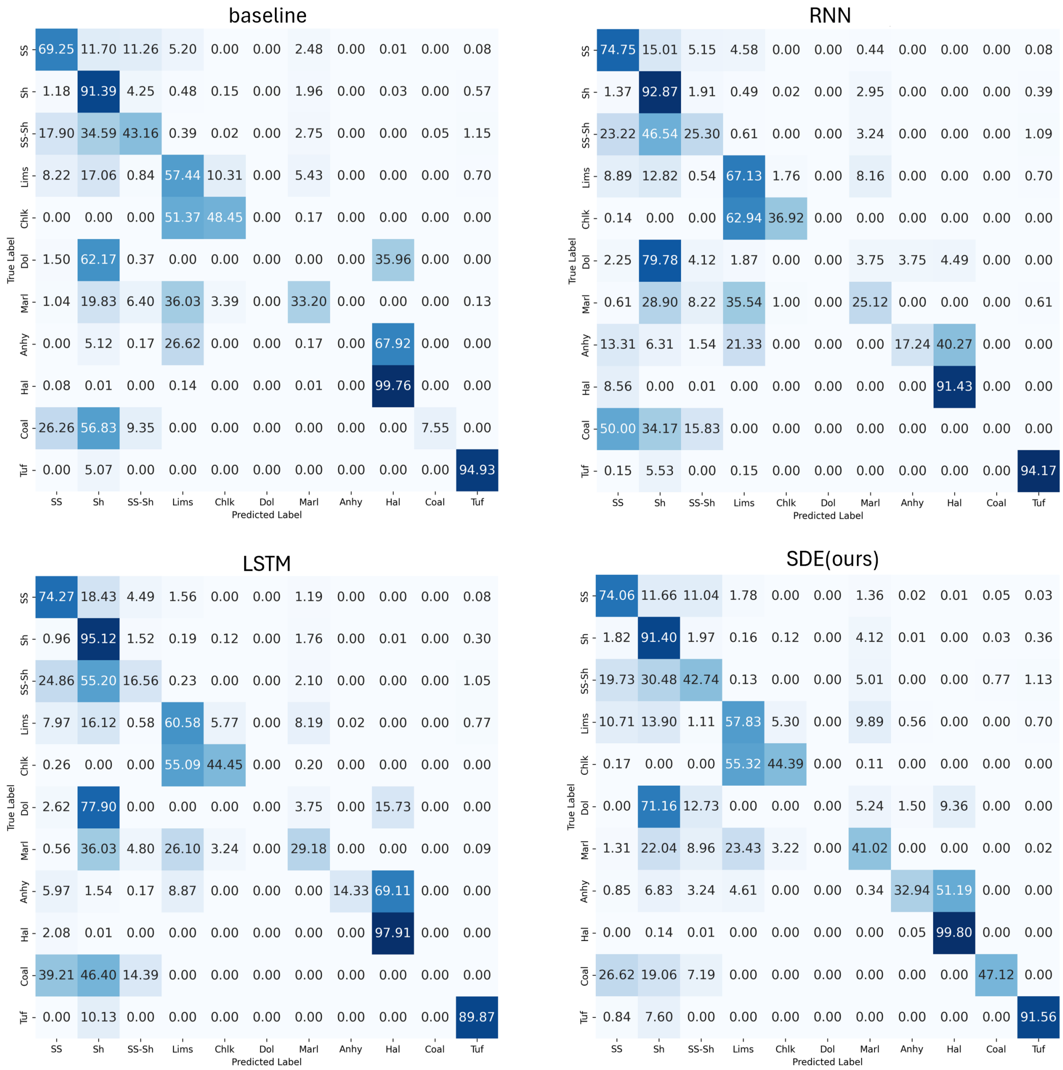

Figure 5. Confusion matrices of lithology classification results for different models.

ated mask blocks to the available logging curves until approximately 30% of the available observations are masked. We then train the model to reconstruct the masked intervals based on the remaining visible logging curves. Instead of randomly masking individual points, we apply continuous mask blocks along the depth direction, which can better simulate the missing logging data scenarios common in real-world logging data, where missing measurements typically appear as continuous intervals due to tool failure, borehole conditions, or acquisition limitations. Furthermore, block masking forces the model to learn a broader geological context and cross-logging correlations, rather than relying on local interpolation between adjacent samples.

The quantitative results are summarized in Tab. 2. The results show that the proposed SDE model significantly outperforms the other approaches. Compared with the baseline method, the relative mean absolute error (RMAE) decreases from 0.189 to 0.119. Meanwhile, the coefficient of determination (R^2) increases from around 0.97 to 0.988, indicating a much stronger agreement between the reconstructed logs and the ground truth. Traditional sequential models (RNN and LSTM) slightly improve the result compared with the baseline method. However, their improvements remain limited, which suggests that these models still struggle to capture complex variations within missing intervals.

Method	RMAE $\downarrow$	$R^2 \uparrow$
Baseline	0.189	0.972
RNN	0.178	0.971
LSTM	0.175	0.972
SDE (Ours)	**0.119**	**0.988**

Table 2. Performance comparison between Baseline, RNN, LSTM, and SDE on missing-log reconstruction.

In Fig. 2, the blue curve represents the actual logging curve, and the orange curve represents the reconstructed result. The blue shaded areas represent the masked areas, which are excluded from the model during the entire training and inference process. The results show that the baseline method and the traditional sequence model can recover the overall trend of the logging curves. However, the reconstruction results exhibit significant oversmoothing, especially in the missing interval. As shown in the highlighted area, the predicted curve often fails to reproduce the high-frequency changes present in the actual logging curve. This problem is particularly evident for resistivity logging curves (such as RSHA, RMED, and RDEP), where the baseline method tends to underestimate the peak amplitude and smooth out steep transitions. In contrast, the proposed SDE achieves the best

Method	F1 score	Acc.	Prec.
Baseline	78.54%	79.91%	78.56%
RNN	75.87%	78.44%	76.97%
LSTM	75.44%	78.84%	75.70%
SDE (ours)	**81.17%**	**81.87%**	**81.32%**

Table 3. Comparison of classification performance between baseline and SDE.

reconstruction performance both quantitatively and qualitatively, with the predicted curve closely matching the actual logging curve within the missing interval, and is able to reproduce the local fluctuations and fine-scale changes within the missing interval. For resistivity logging curves such as RMED and RDEP, the SDE model can more accurately recover peak amplitude and sharp transitions, which are key indicators of lithological changes and reservoir properties.

4.3.2 Lithology Identification We also conducted lithological classification experiments using four different encoders. The evaluation matrix is summarized in Tab. 3. The proposed SDE model performed best across all evaluation metrics, achieving an F1 score of 81.17%, accuracy of 81.87%, and precision of 81.32%. Compared to the baseline reconstruction method, the SDE model improved the F1 score by 2.63% and the classification accuracy by 1.96%, indicating that the reconstructed logging curves generated by the SDE model contain more discriminative geological information.

The qualitative results in Fig. 3 and Fig. 4 further demonstrate the superiority of the SDE model. Compared with the baseline, RNN, and LSTM models, SDE produces predictions that are more consistent with the ground truth, exhibiting clearer lithological boundaries and improved stratigraphic continuity. It also achieves more stable predictions in relatively homogeneous formations such as Halite and Tuff, while better capturing gradual transitions in mixed lithologies such as Sandstone, Shale, and Sandstone/Shale.

To further analyze the class-wise performance, the confusion matrices of different models are shown in Fig. 5. Compared with the baseline, RNN, and LSTM models, the proposed SDE exhibits more concentrated distributions along the diagonal, indicating improved classification accuracy across most lithologies. In *FORCE2020* dataset, certain lithologies inherently exhibit strong confusion due to similar petrophysical responses. For example, Sandstone (SS), Shale (Sh), and mixed facies (SS-Sh) show significant overlap in logging signatures, while Limestone (Lims) and Chalk (Chk), as carbonate rocks, are also difficult to distinguish. Marl, as a mixed lithology, further increases classification ambiguity. Despite these challenges, the SDE model significantly reduces such ambiguities, particularly for transitional lithologies and minority classes such as Coal and Halite(Hal), indicating its ability to capture both global dependencies and subtle variations in well log sequences. Moreover, SDE significantly reduces misclassification among transitional lithologies(Sandstone/Shale) and mixed lithologies(Marl), providing a more reliable representation of complex geological relationships.

5. Conclusion

This study proposes a well logging analysis representation learning encoder based on decoupled interaction modeling. This method aims to address the challenges posed by incomplete well logging measurements and complex geological dependencies in well logging data. By separating the interactions between curve direction and depth direction, the encoder can learn more structured representations from multiple well logging sequences, while reducing the complexity of fully coupled feature interactions.

To evaluate the effectiveness of the learned representations, we conducted two tasks: missing well logging reconstruction and lithological classification. Experimental results show that the proposed SDE significantly improves reconstruction accuracy. Furthermore, in the classification task, the SDE-based approach achieves the best performance across all evaluation metrics, including F1 score, accuracy, and precision. Qualitative analysis of multiple wells further demonstrates that the SDE successfully identifies several lithological intervals missed by other methods, indicating that the learned representations retain more discriminative geological features.

Overall, the experimental results confirm that the proposed decoupled SDE can effectively capture depth-related geological patterns and cross-logging correlations, providing robust representations for incomplete well logging data. These representations not only improve reconstruction performance but also enhance downstream geological interpretation tasks.

6. Acknowledgements

This work was conducted as part of the ThermoOptiPlan. The authors acknowledge the financial and research support provided by the German Federal Ministry of Research, Technology and Space (BMFTR).

References

Ao, Y., Li, H., Zhu, L., Ali, S., Zhongguo, Y., 2018. Logging Lithology Discrimination in the Prototype Similarity Space With Random Forest. *IEEE Geoscience and Remote Sensing Letters*, PP, 1-5.

Bormann, P., Aursand, P., Dilib, F., Manral, S., Dischington, P., 2020. Force 2020 well log and lithofacies dataset for machine learning competition.

Corina, A., Hovda, S., 2018. Automatic lithology prediction from well logging using kernel density estimation. *Journal of Petroleum Science and Engineering*, 170, 664-674.

Han, R., Wang, Z., Wang, W., Xu, F., Qian, X., Cui, Y., 2021. Lithology identification of igneous rocks based on XGboost and conventional logging curves, a case study of the eastern depression of Liaohe Basin. *Journal of Applied Geophysics*. https://api.semanticscholar.org/CorpusID:239956024.

He, Y., Li, W., Dong, Z., Zhang, T., Shi, Q., Wang, L., Wu, L., Qian, S., Wang, Z., Liu, Z., Lei, G., 2023. Lithologic Identification of Complex Reservoir Based on PSO-LSTM-FCN Algorithm. *Energies*, 16, 2135.

Jiang, C., Zhang, D., Chen, S., 2021. Lithology identification from well-log curves via neural networks with additional geologic constraint. *GEOPHYSICS*, 86, 1-77.

Li, Z., Deng, S., Hong, Y., Wei, Z., Cai, L., 2024. A novel hybrid CNN–SVM method for lithology identification in shale reservoirs based on logging measurements. *Journal of Applied Geophysics*, 223, 105346.

Li, Z., Wu, Y., Kang, Y., Lv, W., Feng, D., Yuan, C., 2021. Feature-Depth Smoothness Based Semi-Supervised Weighted Extreme Learning Machine for lithology identification. *Journal of Natural Gas Science and Engineering*, 96, 104306.

Liang, H., Chen, H., Guo, J., Bai, J., Jiang, Y., 2022. Research on lithology identification method based on mechanical specific energy principle and machine learning theory. *Expert Systems with Applications*, 189, 116142.

Shan, L., Liu, Y., Tang, M., Yang, M., Bai, X., 2021. CNN-BiLSTM Hybrid Neural Networks with Attention Mechanism for Well Log Prediction. *Journal of Petroleum Science and Engineering*, 205, 108838.

Wang, L., Zhang, H., Li, J., 2020. Lithology identification technology of logging data based on deep learning model. *Journal of Petroleum Science and Engineering*, 195, 107751.

Xu, D., Wang, Y., Wu, S., 2023. Multi-domain masked reconstruction self-supervised learning for lithology identification using well-logging data. *Engineering Applications of Artificial Intelligence*, 120, 105866.

Ye, Z., Guo, S., Chen, D., Wang, H., Li, S., 2021. Drilling formation perception by supervised learning: Model evaluation and parameter analysis. *Journal of Natural Gas Science and Engineering*, 90, 103923.

Zeng, L., Ren, W., Shan, L., 2020. Attention-Based Bidirectional Gated Recurrent Unit Neural Networks for Well Logs Prediction and Lithology Identification. *Neurocomputing*, 414.

Zhang, P., Ren, J., Zhao, F., Li, X., Zhao, Y., Zhang, C., 2025. LMAFNet: Lightweight multi-scale adaptive fusion network with vertical reservoir information for lithology identification. *Geoenergy Science and Engineering*, 249, 213762.

Zhao, Q., Li, W., He, J., 2022. STNet: Advancing lithology identification with a spatiotemporal deep learning framework for well logging data. *Marine and Petroleum Geology*, 139, 105545.